AD_____

Award Number: W81XWH-11-1-0763

TITLE: Anti-NGF Local Therapy for Autonomic Dysreflexia in Spinal Cord Injury

PRINCIPAL INVESTIGATOR: Naoki Yoshimura

CONTRACTING ORGANIZATION: University of Pittsburgh
Pittsburgh, PA 15213-3320

REPORT DATE: October 2012

TYPE OF REPORT: Annual

PREPARED FOR: U.S. Army Medical Research and Materiel Command
Fort Detrick, Maryland 21702-5012

REPORT DOCUMENTATION PAGE

Form Approved
OMB No. 0704-0188

1. REPORT DATE	2. REPORT TYPE	3. DATES COVERED
October 1, 2012	Annual	09/30.2011-09/29/2012

4. TITLE AND SUBTITLE
Anti-NGF Local Therapy for Autonomic Dysreflexia in Spinal Cord Cord Injury

5a. CONTRACT NUMBER

5b. GRANT NUMBER
W81XWH-11-1-0763

5c. PROGRAM ELEMENT NUMBER

6. AUTHOR(S)
Naoki Yoshimura

E-Mail: nyos@pitt.edu

5d. PROJECT NUMBER

5e. TASK NUMBER

5f. WORK UNIT NUMBER

7. PERFORMING ORGANIZATION NAME(S) AND ADDRESS(ES)
University of Pittsburgh
Pittsburgh, PA 15213-3320

8. PERFORMING ORGANIZATION REPORT NUMBER

9. SPONSORING / MONITORING AGENCY NAME(S) AND ADDRESS(ES)
U.S. Army Medical Research and Materiel Command
Fort Detrick, Maryland 21702-5012

10. SPONSOR/MONITOR'S ACRONYM(S)

11. SPONSOR/MONITOR'S REPORT NUMBER(S)

12. DISTRIBUTION / AVAILABILITY STATEMENT
Approved for Public Release; Distribution Unlimited

13. SUPPLEMENTARY NOTES

14. ABSTRACT
Autonomic dysreflexia (AD), which induces excessive elevation of blood pressure, is a potentially life-threatening medical emergency that occurs in persons with spinal cord injury (SCI) at or above the mid-thoracic spinal cord segment. Since the most common source of stimulation that initiates AD is the genitourinary tract including bladder distention, followed by colorectal distension, elimination of activation of bladder sensory pathways during bladder distention could significantly reduce the incidence and/or degree of AD in SCI. Because previous studies have indicated that increased levels of nerve growth factor (NGF) in sensory pathways are one of the key factors to induce increased excitability of sensory pathways after SCI, anti-NGF therapy could be an attractive treatment of AD in SCI patients. However, systemic anti-NGF treatment such as the use of NGF antibodies reportedly induces some side effects. Therefore, we hypothesize that the local therapy of NGF antisense delivery using liposomes (LPs) in the bladder could reduce the activation of bladder sensory pathways, thereby suppressing AD during bladder distention after SCI. Using adult female rats with chronic spinal cord injury induced by Th4 spinal cord transection, we will investigate: (1) the contribution of hyperexcitable bladder sensory pathways in the emergence of AD in SCI (Aim 1), and (2) the effects of intravesical delivery of NGF antisense-liposome conjugate, which reduce NGF expression in the bladder, on AD in SCI (Aim 2). If successfully completed, this study directly addresses the feasibility of local NGF antisense treatment for SCI-induced AD and provides the foundation for future clinical translation of local NGF antisense therapy in military service members, their family members, and/or the U.S. veteran population, who suffer from autonomic dysreflexia due to SCI. The local anti-NGF therapy could also be extended to a general population of people with SCI or other spinal cord lesions such as multiple sclerosis. The long-term objectives of the research program are to establish new and effective therapeutic targets and/or interventions strategies for the treatment of vascular complications of SCI.

15. SUBJECT TERMS
Anti-NGF Local Therapy

16. SECURITY CLASSIFICATION OF:			17. LIMITATION OF ABSTRACT	18. NUMBER OF PAGES	19a. NAME OF RESPONSIBLE PERSON
a. REPORT	b. ABSTRACT	c. THIS PAGE			USAMRMC
U	U	U	UU	17	19b. TELEPHONE NUMBER *(include area code)*

Table of Contents

I. Introduction

Autonomic dysreflexia (AD), which induces excessive elevation of blood pressure, is a potentially life-threatening medical emergency that occurs in persons with spinal cord injury (SCI) at or above the mid-thoracic spinal cord segment. The most common source of stimulation that initiates AD is the genitourinary tract including bladder distention. Therefore, the purpose of this project is to investigate the feasibility of local nerve growth factor (NGF) antisense treatment for SCI-induced AD during bladder distention and provides the foundation for future clinical translation of local NGF antisense therapy in people with SCI-induced AD.

II. Body

II.1. Timeline described in the SOW: PITT: University of Pittsburgh

<table>
<tr><td></td><td colspan="3">Year 1</td><td colspan="3">Year 2</td><td colspan="2">Year 3</td><td></td></tr>
<tr><td></td><td>0-2mo</td><td>3-8mo</td><td>9-12mo</td><td>13-16mo</td><td>17-20mo</td><td>21-24mo</td><td>25-28mo</td><td>29-32mo</td><td>33-36mo</td></tr>
<tr><td rowspan="2">AIM 1 (PITT)</td><td>Regulatory approval for animal research</td><td colspan="2">□ Order animals/
□ Prepare protocols/ documentation
□ Comparison of blood pressure responses during bladder distention between spinal intact and SCI rats</td><td colspan="2">□ Comparison of blood pressure responses during bladder distention in SCI rats with or without capsaicin pretreatment
□ Comparison of electrophysiological properties of bladder afferent neurons from spinal intact and SCI rats
□ Tissue analysis
ELISA
histology</td><td colspan="2">Animal study data analysis/ reporting</td><td colspan="2"></td></tr>
<tr><td></td><td colspan="4">□ Tissue analysis
Optimization and analysis of NGF expression using molecular techniques such as PCR and ELISA in spinal intact and SCI rats</td><td colspan="2">Data analysis/ reporting of NGF expression data</td><td colspan="2"></td></tr>
<tr><td rowspan="2">AIM 2 (PITT)</td><td colspan="3"></td><td colspan="3">□ Comparison of blood pressure responses during bladder distention in SCI rats with or without NGF antisense treatment
□ Comparison of dosing strategy using one-time or twice application of LP-anti NGF for reducing of blood pressure responses
□ Comparison of effects of cationic liposomes vs. amphoteric liposomes (charge-reversible character) on blood pressure responses
□ Tissue analysis
ELISA
histology</td><td colspan="2">□ Comparison of electrophysiological properties of bladder afferent neurons from SCI rats with or without NGF antisense treatment</td><td>Data analysis/ reporting</td></tr>
<tr><td colspan="3">□ Optimize formulation of NGF antisense
□ Manufacture LPs
□ Analytical method development</td><td colspan="5">□ Develop LP-NGF antisense using cationic and amphoteric liposomes
□ Tissue analysis
Analysis of NGF expression using molecular techniques such as PCR and ELISA in SCI rats with LP-NGF antisense treatment</td></tr>
</table>

II-2. Research Accomplishments

Aim 1 (Year 1)

- *Regulatory approval for animal research*
- *Order animals*
- *Prepare protocols/ documentation*

[Accomplishment]

We have obtained required approvals for the animal protocol from the University of Pittsburgh IACUC and the US Army Medical Research and Materiel Command (USAMRMC) Animal Care and Use Review Office (ACURO) before starting the project and animal orders.

- *Comparison of blood pressure responses during bladder distention between spinal intact and spinal cord injury (SCI) rats*

[Accomplishment]

In the first year of the project, we performed experiments to measure blood pressure responses during bladder distention using normal rats and rats with Th4-level spinal cord transection (4 weeks). In order to evaluate autonomic dysreflexia (AD) after SCI, the bladder-to-vascular responses during bladder distention was examined under urethane anesthesia. For bladder distention, intravesical pressure was increased in a stepwise manner (20–100 cmH_2O with 20 cmH_2O increments, for 2 min, at 2-min intervals) by connecting the urethra cannula through a three-way stopcock to a saline-filled reservoir, the height of which was adjusted to maintain a constant pressure in the bladder.

We have found that: (1) arterial blood pressure was increased during bladder distention in an intravesical pressure-dependent manner in spinal intact and SCI rats (Fig. 1), and (2) the increase in arterial blood pressure during bladder distention in SCI rats started occurring at low intravesical pressure (20 cmH_2O) compared with spinal intact rats, in which the arterial blood pressure increase at 20 cmH_2O of intravesical pressure was negligible (Table 1). These results indicate that SCI (4 weeks) induced AD as evidenced by the earlier onset of arterial blood pressure elevation during bladder distention in SCI rats vs. spinal intact rats.

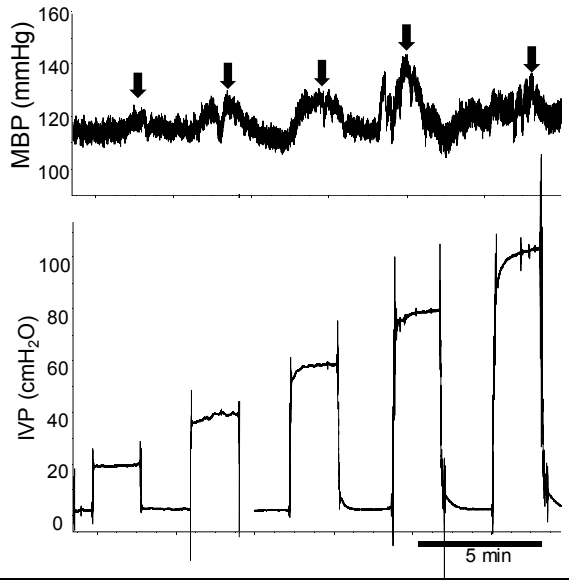

Fig. 1. Arterial blood pressure responses during passive bladder distention from 20 to 100 cmH_2O with 20 cmH_2O increments, for a duration of 2 min each at 2 min intervals in a spinal cord inured (SCI) rat. MBP: mean blood pressure. IVP: intravesical pressure. Arrows in the upper chart indicate the peak blood pressure responses during intravesical pressure elevation (lower chart).
Note that blood pressure responses started being seen at 20 cmH_2O bladder distension and increased in a bladder pressure-dependent manner up to 80 cmH_2O.

TABLE 1. Correlation between arterial blood pressure and bladder pressure in spinal intact and SCI rats

	Bladder pressure			
	20 cmH_2O	40 cmH_2O	60 cmH_2O	80 cmH_2O
Blood pressure (mmHg)				
Intact (n=5)	4.3 ± 1.3	15.4 ± 1.3	25.2 ± 3.8	32.5 ± 3.1
SCI (n=5)	10.2 ± 0.8 *	13.2 ± 1.3	14.0 ± 1.6	19.9 ± 1.8

Data: mean ± S.E. *P<0.05 vs. Intact (spinal intact rats)

- *Tissue analysis: Optimization and analysis of NGF expression using molecular techniques such as PCR and ELISA in spinal intact and SCI rats*

[Accomplishment]
We successfully performed ELISA experiments to measure NGF protein levels separately in the mucosa and detrusor layer of the bladder of spinal intact and SCI rats. We have found the increased levels of NGF in the mucosa and detrusor of the bladder after SCI (Table 2).

TABLE 2. NGF protein levels of the bladder (mucosa and detrusor) in spinal intact and SCI rats

	Intact (n=5)		SCI (n=5)	
	Mucosa	Detrusor	Mucosa	Detrusor
NGF (pg/mg tissue protein)	1705.3 ± 134.7	1921.3 ± 195.3	3986.4 ± 630.4*	2659.2 ± 459.6*

Data: mean ± S.E. *P<0.05 vs. the corresponding sites (mucosa or detrusor) of the Intact group (spinal intact rats)

- *Comparison of electrophysiological properties of bladder afferent neurons from spinal intact and SCI rats*
- *Tissue analysis (histology) of dorsal root ganglion (DRG) neurons*

[Accomplishment]
We performed the electrophysiological experiments using patch-clamp recordings and histological analyses of DRG neuron including those innervating the urinary bladder. In patch clamp recordings, we used dissociated DRG neurons innervating the bladder from spinal intact and SCI rats, which were identified by axonal transport of fluorescent dyes, Fast Blue, injected into the bladder 1 week before experiments. Dissociated DRG neurons were obtained by enzymatic methods from L6-S1 DRG (Hayashi et al., 2009). We examine action potential characteristics including spike thresholds and firing pattern (current clamp conditions) in capsaicin-sensitive C-fiber afferent neurons in order to evaluate C-fiber afferent hyperexcitability after SCI.

We have found that: (1) capsaicin-sensitive bladder afferent neurons from SCI rats exhibited lower thresholds for spike activation (-26.4±1.3mV) than those from control rats (-21.8±0.9mV) and did not exhibit membrane potential relaxation during membrane depolarization (Fig. 2A), (2) the number of firing during a 800 msec depolarizing pulse was significantly increased after SCI (4.7±0.7 spikes, n=19 cells) compared to control rats (1.3±0.1 spikes, n=20 cells) (Fig. 2A), and that the peak density of A-type potassium (K_A) currents during membrane depolarization to 0mV in capsaicin-sensitive B-AN of SCI rats was significantly smaller (38.1±4.6 pA/pF, n=22 cells) than that from control rats (68.6±6.3 pA/pF, n=19 cells) (Fig. 2B) (Takahashi et al., 2012 [2012 AUA abstract; PDF file included]). These results indicate that SCI induces hyperexcitability of capsaicin-sensitive C-fiber bladder afferent neurons due to reduced K_A channel activity after SCI

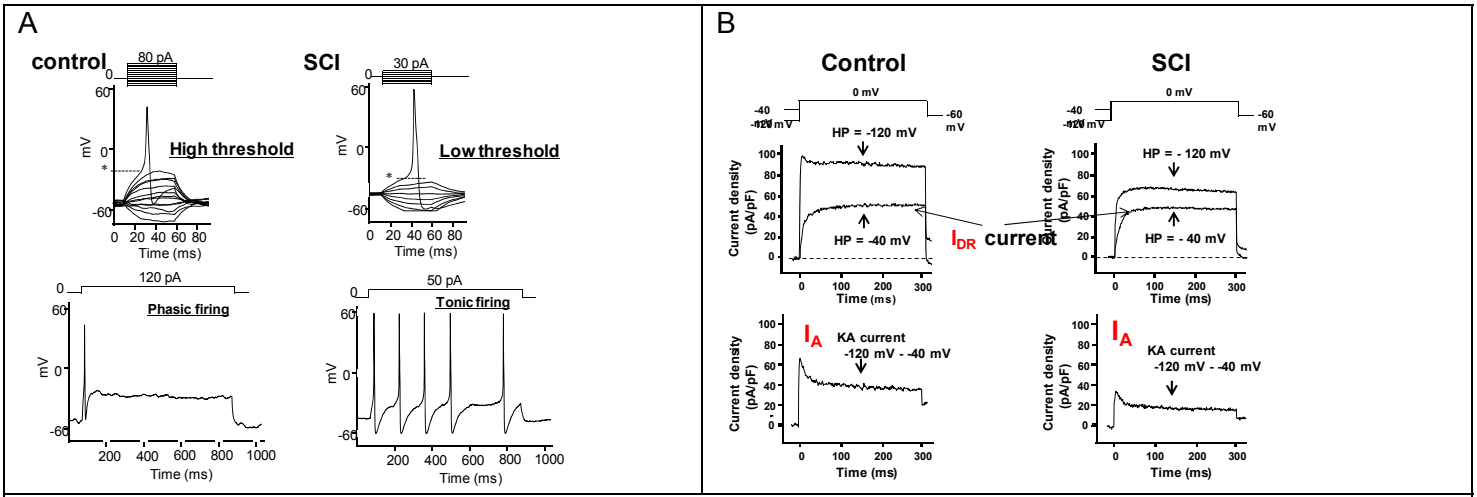

Fig. 2. Electrophysiological properties of capsaicin-sensitive bladder afferent neurons from spinal intact (Control) and SCI rats. A: Changes in firing characteristics of capsaicin-sensitive bladder afferent DRG neurons following SCI. Upper panels show action potentials evoked by 50 msec depolarizing current pulses injected through patch pipettes in a current-clamp condition. Lower panels show firing patterns during membrane depolarization (800 msec of duration). The pulse protocols are shown in the insets. Note the lower threshold for spike activation and repetitive firing pattern in the bladder afferent neuron from SCI rats compared to control rats. B: Changes in K^+ currents of capsaicin-sensitive bladder afferent DRG neurons following SCI. Inward currents were suppressed by equimolar substitution of choline for Na^+ and reduction of Ca^{2+} in the external solution. Upper panels show superimposed outward K^+ currents evoked by voltage steps to 0 mV

from holding potentials of –120 and –40 mV. Lower panels show A-type K^+ currents (I_A) obtained by subtraction of the K^+ currents evoked by depolarization to 0 mV from holding potentials of –40 and –120 mV. Note a reduction in K_A current amplitudes in capsaicin-sensitive bladder afferent neurons from SCI rats although sustained delayed rectifier (K_{DR}) current (I_{DR}) was not altered.

Based on these findings of patch clamp recordings, we also performed histological experiments to examine the expression of Kv4 family Kv channel subunits (Kv4.1, Kv4.2 and Kv4.3) and their auxiliary subunits because they comprise K_A channel in DRG neurons (Matsuyoshi et al., 2012 [PDF file included]). Using immunohistochemistry, *in situ* hybridization and RT-PCR technique, we have found that: (1) the two pore-forming subunits Kv4.1 and Kv4.3 show distinct cellular distributions; that is, Kv4.3 is predominantly in isolectin b4-positive, small-sized C-fiber neurons, whereas Kv4.1 is seen in DRG neurons in various sizes although Kv4.2 was not expressed in DRG neurons and (2) the two classes of Kv4 channel auxiliary subunits are also distributed in different-sized cells; that is, KChIP3 is the only significantly expressed Ca^{2+}-binding cytosolic ancillary subunit in DRGs and present in medium to large-sized neurons whereas the membrane-spanning auxiliary subunit DPP6 is seen in a large number of DRG neurons in various sizes, whereas DPP10 is restricted in small-sized neurons (please see the detail in the paper by Matsuyoshi et al., 2012 [PDF file included]).

These results indicate that Kv4.3 and DPP10 may contribute to A-type K^+ currents in non-peptidergic, C-fiber somatic afferent neurons. Because we previously reported that the population of isolectin B4-posiitve, non-peptidergic cells among C-fiber afferent DRG neurons is numerically smaller in bladder afferent neurons compared to somatic afferent neurons (Yoshimura et al., 2003) and that Kv1.4, which is another Kv subunit comprising K_A channels, is decreased to induce C-fiber afferent hyperexcitability in rat with chemical cystitis (Hayashi et al., 2009), it is assumed that KV4.3 subunit contributes to K_A current in somatic afferent neurons whereas Kv1.4 subunit is involved in the formation of K_A channels in visceral afferent neurons including those innervating the bladder. We will further try to characterize the properties of ion channels and their changes in bladder afferent neurons using SCI rats in the second year of the project.

Aim 2 (Year 1)

- *Optimize formulation of NGF antisense*
- *Manufacture LPs*
- *Analytical method development*

[Accomplishment]

In the first year of the project, we optimized and manufactured liposomes (LPs) conjugated with NGF antisense as follows. The 18mer phosphorothioate oligodeoxynucleotide (ODN) with the sequence 5'-GCCCGAGACGCCTCCCGA-3' for the experiments were made, and cationic liposomes composed of DOTAP (N-[1-(2,3-Dioleoyloxy)propyl]-N,N,N trimethylammonium methylsulfate) were made by thin film hydration method and hydrated with nuclease free water with the final lipid concentration of 7mM. The ODN were dissolved in nuclease free water at the concentration of 2mM and were complexed with liposomes in the proportion of 6μl ODN solution to 1 ml liposome lipid by incubation at room temperature for 30min.

Then, we perform in-vivo experiments to develop the analytical method to test the efficacy of LPs conjugated with NGF antisense. Rats were anesthetized with 2% isoflurane, and catheterized by a 24-gauge angiocatheter through the urethra into the bladder. After urine was drained from the bladder, 12μM of NGF antisense or scramble OND complexed with liposome or saline in a volume of 0.5ml was infused. The bladder outlet was tied with a running suture thread for 30 minutes. Then rats were released from the tighten thread and allowed to recover from the anesthesia. The efficacy of LP-antisense treatments was assessed 24h after infusion by saline and subsequent acetic acid (AA) cystometry under urethane anesthesia (1.0 g/kg, s.c.). A polyethylene catheter (PE-50) connected by a three-way stopcock to a pressure transducer and to a syringe pump was then inserted into the bladder through the dome for recording intravesical pressure and infusing solutions into the bladder. The intravesical pressure was recorded with a data-acquisition software (sampling rate 400 Hz; Chart) on a computer system equipped with an analog-to-digital converter. A control cystometrogram (CMG) was performed by slowly filling the bladder with saline (0.04 mL/min) to elicit repetitive voiding more than for 1 hour followed by 0.25% acetic acid (AA) infusion to induce bladder irritation for more than 3 hours. The intercontractile interval (ICI) of the reflex bladder contractions during saline and AA was measured. The ICI duration was determined as the time between 2 continuing contraction cycles. The

average of ICI during saline and AA infusion was obtained the average of at least 3 ICIs measured more than 30 min after saline infusion and 60 min after AA infusion, respectively.

We have found that; (1) LPs conjugated with NGF antisense were retained in the urothelium after intravesical application as evidenced by histological identification of LP antisense tagged with a fluorescent dye (Fig. 3), (2) LPs-NGF antisense treatment suppressed AA-induced bladder oveactivity as evidenced by the reduction in the ICI decrease after intravesical AA application in the LPs-NGF-treated groups vs. control groups (saline or LPs-scramble oligo treatment) (Fig. 4), and (3) LPs-NGF antisense treatment reduced the NGF expression in the bladder mucosal layer (Table 3). These results indicate that the manufactured LPs-NGF antisense conjugate is effective to suppress the urothelial NGF expression and inhibit bladder overactivity induced by bladder afferent sensitization. Thus, we expect that this formula of LPs-NGF antisense conjugate will be effective to suppress AD during bladder distention in SCI animals, which will be tested in the second year of the project.

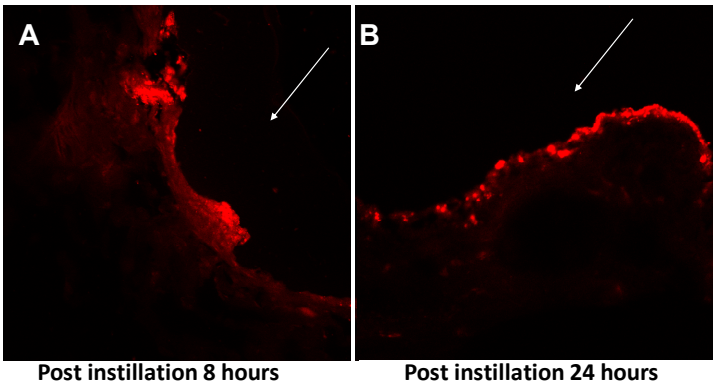

Fig.3. Confocal images of harvested rat bladders at 8 (panel A) and at 24 hours (panel B) after instillation of liposomal antisense with 5' tag of TYETM 563. The red fluorescence in panels A represents successful bladder distribution of ODN at 8h and the fluorescence seems to be more concentrated due to bladder folds. The bright red fluorescence was more homogenous in the urothelium at 24h with diffusion to cells in deeper layers (panel B). Localization of fluorescence in urothelium demonstrates successful uptake and retention in target cells due to binding with target mRNA. Lumen side of the section is marked by white arrow. Magnification is 40x in all sections.

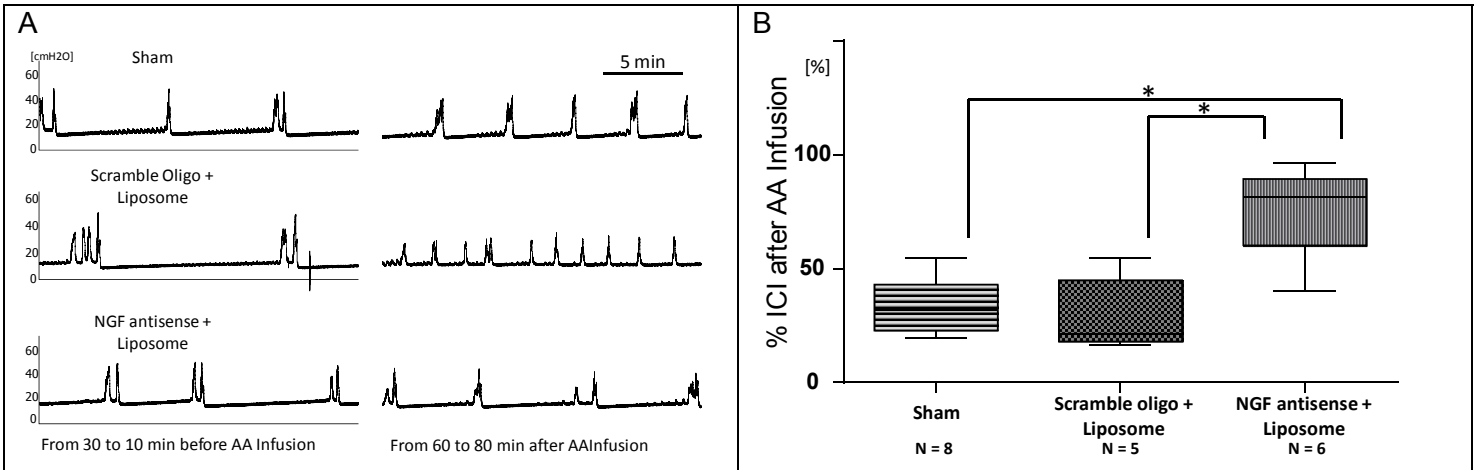

Fig. 4. Cystometric analysis of the effects of liposome (LP)-NGF antisense treatment on bladder overactivity induced by intravesical application of acetic acid (AA; 0.25%) in rats. A: Representative cystometrograms showing the effects of intravesical application of AA in sham (saline treatment) (upper traces), LP-scramble oligo-treated (middle traces) and LP-NGF antisense treated rats (lower traces). The cystometrograms before (30 to 10 min before AA application) and after (60-90 min after AA application) are shown in left and right traces, respectively. Note that the AA-induced reduction in intercontraction intervals (ICI) was seen in sham and scramble oligo-treated rats, but not in the rat treated with LP-NGF antisense conjugates.
B: Changes in ICIs after intravesical AA application expressed as the percent ratio of ICI after AA application against the ICI values prior to AA application. Note that the AA-induced reduction of ICI was significantly smaller in the LP-NGF antisense treated group (n=6) compared to sham (saline-treated) (n=8) and LP-scramble oligo-treated groups (n=5). *p<0.05 compared to sham or scramble oligo groups

TABLE 3. Effects of LP-NGF antisense treatment on NGF expression after acetic acid (AA) application in the mucosal layer of SCI rat bladders (ELISA)

	Control (no AA) (n=5)	Sham (n=4)	LP- NGF antisense (n=4)
NGF (pg/mg tissue protein)	1043.8 ± 116.0	3847.7 ± 736.4*	1415.9 ± 175.1#

Data: mean ± S.E. *P<0.05 vs. Control, #P<0.05 vs. Sham

III. Key research accomplishments

- Preparation and approval of animal protocols/documentation
- Detection of autonomic dysreflexia (AD) during bladder distention in SCI rats
- Detection of increased NGF expression in the bladder of SCI rats
- Detection of hyperexcitability of bladder afferent neurons due to the reduction of A-type K^+ channel activity in SCI rats
- Characterization of differential distribution of Kv4 channel subunits in DRG neurons
- Formulation and optimization of liposomes-NGF antisense conjugates
- Development of analytical methods to confirm the effectiveness of formulated liposomes-NGF antisense conjugates

IV. Reportable outcomes

Published abstract:

1. Takahashi, R., Yunoki, T., Naito, S., Yoshimura, N.: Increased excitability of bladder afferent neurons in rats with spinal cord injury: a role of A-type voltage-gated potassium channels. 110th Annual Meeting AUA, Abstract No. 38, Atlanta, GA, May 19-23, 2012.

Refereed article:

1. Matsuyoshi, H., Takimoto, K., Yunoki, T., Erickson, V.L., Tyagi, P., Hirao, Y., Wanaka, A., Yoshimura, N.: Distinct cellular distributions of Kv4 pore-forming and auxiliary subunits in rat dorsal root ganglion neurons. Life Sciences, in press, 2012.

V. Conclusions

In the first year of the project, we successfully completed the works listed in the SOW (Year 1). Base on the results obtained in the first year of the funding period, we observed two major implications for the SCI research. First, our results indicate that SCI induces autonomic dysreflexia (AD) during bladder distention as evidenced by enhanced arterial pressure responses during low-pressure bladder distention in SCI rats. Secondly, our formulation of liposomes conjugated with NGF antisense successfully suppresses bladder overactivity induced by AA-induced C-fiber sensitization in association with the reduction in NGF expression in the bladder urothelium. In the second year of the project, we will continue to investigate the pathogenesis of SCI-induced AD and the therapeutic effects of liposome-NGF antisense conjugates on SCI-induced AD, as proposed in the SOW (Year 2 timeline).

VI. References

Hayashi, Y., Takimoto, K., Chancellor, M.B., Erickson, K.A., Erickson, V.L., Kirimoto, T., Nakano, K., de Groat, W.C., Yoshimura, N.: Bladder hyperactivity and increased excitability of bladder afferent neurons associated with reduced expression of Kv1.4 □-subunit in rats with cystitis. American Journal of Physiology Regulatory, Integrative and Comparative Physiology, 296: R1661-1670, 2009.

Matsuyoshi, H., Takimoto, K., Yunoki, T., Erickson, V.L., Tyagi, P., Hirao, Y., Wanaka, A., Yoshimura, N.: Distinct cellular distributions of Kv4 pore-forming and auxiliary subunits in rat dorsal root ganglion neurons. Life Sciences, in press, 2012.

Takahashi, R., Yunoki, T., Naito, S., Yoshimura, N.:: Increased excitability of bladder afferent neurons in rats with spinal cord injury: a role of A-type voltage-gated potassium channels. 110th Annual Meeting AUA, Abstract No. 38, Atlanta, GA, May 19-23, 2012.

Yoshimura, N., Seki, S., Erickson, K.A., Erickson, V.L., Chancellor M.B. and de Groat, W.C.: Histological and electrical properties of rat dorsal root ganglion neurons innervating the lower urinary tract. Journal of Neuroscience, 23: 4355-4561, 2003.

VII. Appendices

PDF files of the following publications are appended.

1. Takahashi, R., Yunoki, T., Naito, S., Yoshimura, N.:: Increased excitability of bladder afferent neurons in rats with spinal cord injury: a role of A-type voltage-gated potassium channels. 110th Annual Meeting AUA, Abstract No. 38, Atlanta, GA, May 19-23, 2012.
2. Matsuyoshi, H., Takimoto, K., Yunoki, T., Erickson, V.L., Tyagi, P., Hirao, Y., Wanaka, A., Yoshimura, N.: Distinct cellular distributions of Kv4 pore-forming and auxiliary subunits in rat dorsal root ganglion neurons. Life Sciences, in press, 2012.

1202631

Increased excitability of bladder afferent neurons in rats with spinal cord injury: a role of A-type voltage-gated potassium channels

Ryosuke Takahashi, Pittsburgh, PA; Seiji Naito, Fukuoka, Japan; Naoki Yoshimura, Pittsburgh, PA

INTRODUCTION AND OBJECTIVE: Although the etiology of overactive bladder (OAB) seems to be mutifactorial, afferent sensitization is considered to contribute to OAB symptoms such as urgency. Also, increased excitability of C-fiber afferent pathways has been proposed as an important pathophysiological basis of neurogenic detrusor overactivty (DO) in humans and animals with spinal cord injury (SCI). However, the functional mechanisms inducing hyperexcitability of C-fiber bladder afferent neurons (B-AN) after SCI are not fully elucidated. We therefore examined changes in electrophysiological properties of B-AN obtained from SCI rats, especially focusing on voltage-gated potassium channels, using patch-clamp recording techniques.

METHODS: SCI was produced by transection of the spinal cord at the level of T9-T10 in female SD rats. After 4 weeks, L6-S1 dorsal root ganglia (DRG) were removed from spinal intact and SCI rats, and freshly dissociated DRG neurons were prepared with enzymatic methods. Whole cell patch-clamp recordings were performed on individual B-AN, which were labeled by retrograde axonal transport of a fluorescent dye, Fast Blue (FB), injected into the bladder wall 7 days earlier and identified with a fluorescent microscope. Since the majority of C-fiber B-AN are sensitive to capsaicin, FB-labeled cells that exhibited inward currents in response to capsaicin (500nM) application were selected for evaluation.

RESULTS: Capsaicin-sensitive B-AN from SCI rats exhibited lower thresholds for spike activation (-26.4±1.3mV) than those from control rats (-21.8±0.9mV) and did not exhibit membrane potential relaxation during membrane depolarization. The number of firing during a 800 msec depolarizing pulse was significantly increased after SCI (4.7±0.7 spikes) compared to control rats (1.3±0.1 spikes). The peak density of A-type potassium (K_A) currents during membrane depolarizations to 0mV in capsaicin-sensitive B-AN of SCI rats was significantly smaller (38.1±4.6 pA/pF) than that from control rats (68.6±6.3 pA/pF), and the inactivation curve of the K_A current was displaced to more hyperpolarized levels by ~10mV after SCI. On the other hand, the sustained delayed-rectifier potassium current density was not altered after SCI.

CONCLUSIONS: These results suggest that reduced K_A channel activity in involved in hyperexcitability of capsaicin-sensitive C-fiber B-AN after SCI. Thus, the K_A channel could be a potential target for treating OAB due to neurogenic DO.

Source of funding: NIH DK57267, DK68557 and DOD SC100134

Life Sciences xxx (2012) xxx–xxx

Contents lists available at SciVerse ScienceDirect

Life Sciences

journal homepage: www.elsevier.com/locate/lifescie

Distinct cellular distributions of Kv4 pore-forming and auxiliary subunits in rat dorsal root ganglion neurons

Hiroko Matsuyoshi [b], Koichi Takimoto [c], Takakazu Yunoki [a], Vickie L. Erickson [a], Pradeep Tyagi [a], Yoshihiko Hirao [d], Akio Wanaka [e], Naoki Yoshimura [a,*]

[a] Department of Urology, School of Medicine, University of Pittsburgh; Pittsburgh, Pennsylvania 15213, USA
[b] Department of Physiology II, Faculty of Medicine, Nara Medical University; Kashihara, Nara 634-8521, Japan
[c] Department of Bioengineering, Nagaoka University of Technology, Nagaoka, 940-2188, Japan
[d] Department of Urology, Faculty of Medicine, Nara Medical University; Kashihara, Nara 634-8521, Japan
[e] Department of Anatomy & Neuroscience, Faculty of Medicine, Nara Medical University; Kashihara, Nara 634-8521, Japan

ARTICLE INFO

Article history:
Received 18 March 2012
Accepted 7 July 2012
Available online xxxx

Keywords:
Dorsal root ganglion
Voltage-gated potassium channel
Kv4.1
KChIP
DPP

ABSTRACT

Aims: Dorsal root ganglia contain heterogeneous populations of primary afferent neurons that transmit various sensory stimuli. This functional diversity may be correlated with differential expression of voltage-gated K^+ (Kv) channels. Here, we examine cellular distributions of Kv4 pore-forming and ancillary subunits that are responsible for fast-inactivating A-type K^+ current.

Main methods: Expression pattern of Kv α-subunit, β-subunit and auxiliary subunit was investigated using immunohistochemistry, *in situ* hybridization and RT-PCR technique.

Key findings: The two pore-forming subunits Kv4.1 and Kv4.3 show distinct cellular distributions: Kv4.3 is predominantly in small-sized C-fiber neurons, whereas Kv4.1 is seen in DRG neurons in various sizes. Furthermore, the two classes of Kv4 channel auxiliary subunits are also distributed in different-sized cells. KChIP3 is the only significantly expressed Ca^{2+}-binding cytosolic ancillary subunit in DRGs and present in medium to large-sized neurons. The membrane-spanning auxiliary subunit DPP6 is seen in a large number of DRG neurons in various sizes, whereas DPP10 is restricted in small-sized neurons.

Significance: Distinct combinations of Kv4 pore-forming and auxiliary subunits may constitute A-type channels in DRG neurons with different physiological roles. Kv4.1 subunit, in combination with KChIP3 and/or DPP6, form A-type K^+ channels in medium to large-sized A-fiber DRG neurons. In contrast, Kv4.3 and DPP10 may contribute to A-type K^+ current in non-peptidergic, C-fiber somatic afferent neurons.

Introduction

Voltage-gated K^+ (Kv) currents in sensory neurons are divided into two major categories; sustained delayed rectifier (K_{DR}) and transient A-type K^+ (K_A) currents (Kostyuk et al., 1981; Hall et al., 1994; Gold et al., 1996; Yoshimura et al., 1996). K_A current is activated at subthreshold of action potential and rapidly inactivates. Thus, this current is important to determine the initiation and interval of action potentials. K_A current in sensory neurons may be carried by a number of Kv pore-forming subunits including Kv1.4 and any of Kv4 subunits (Kv4.1, Kv4.2, and Kv4.3). It has been shown that Kv1.4 is localized in small-sized C-fiber DRG neurons (Rasband et al., 2001). Furthermore, K_A current in small-sized C-fiber neurons exhibits slower inactivation and sensitivity to α-dendrotoxin, a blocker of Kv1-family channels. In addition, reduced K_A current and Kv1.4 proteins are associated with hyperexcitability of DRG neurons in animal models of bladder pain (Hayashi et al., 2009). Therefore, Kv1.4 significantly contributes to the formation of A-type channels in a subset of C-fiber neurons. In contrast to Kv1.4 subunits, relatively less is known about cellular distributions of Kv4 channel subunits in DRGs. Previous studies showed that Kv4.3 protein is predominantly expressed in non-peptidergic, small-sized DRG neurons (Chien et al., 2007). PCR analysis also detected Kv4.1 mRNA in DRG tissue and a large number of isolated, small to medium-sized DRG neurons (Phuket and Covarrubias, 2009). These findings support differential expression of the two Kv4 pore-forming subunits in distinct DRG neurons. Yet, the cell-size distribution of Kv4.1 in the entire DRG neuronal population remains unclear.

Kv4 pore-forming proteins are known to form complexes with two distinct types of auxiliary subunits that markedly alter channel expression and gating. The first type of Kv4 auxiliary subunits are small cytosolic Ca^{2+}-binding proteins, namely Kv channel interacting proteins (KChIPs) (An et al., 2000), whereas the other type contains one transmembrane domain with a large extracellular portion similar to dipeptidyl peptidase (DPP6/10) (Jerng et al., 2004; Nadal et al., 2003; Ren et al., 2005). Diverse KChIPs are generated by the presence

* Corresponding author at: Department of Urology, University of Pittsburgh School of Medicine, Suite 700 Kaufmann Medical Building, 3471 Fifth Ave., Pittsburgh, Pennsylvania 15213, USA. Tel.: +1 412 692 4137; fax: +1 412 692 4380.
E-mail address: nyos@pitt.edu (N. Yoshimura).

0024-3205/$ – see front matter © 2012 Elsevier Inc. All rights reserved.
doi:10.1016/j.lfs.2012.07.007

of four genes (An et al., 2000; Morohashi et al., 2002) and alternative splicing of transcripts (Rosati et al., 2001; Takimoto et al., 2002; Holmqvist et al., 2002; Patel et al., 2002; Boland et al., 2003). However, less is known about the distribution of KChIPs and DPPs in DRG neurons.

We wished to determine cellular distributions and subunit compositions of Kv4 channel complexes in distinct DRG neurons. We utilized PCR analysis, in-situ hybridization and immunohistochemistry to examine the expression and cellular distributions of Kv4 pore-forming and auxiliary subunits in rat DRG neurons.

Materials and methods

Experiments were performed using female Sprangue–Dawley rats (220–250 g). Care and handling of animals were in accordance with institutional guidelines and were approved by the Animal Care and Use Committees of the Nara Medical University and University of Pittsburgh Institutional Animal Care and Use Committees.

PCR analysis

Total RNAs were prepared from L6-S1 DRGs and total brain using a column-based isolation method (Qiagen, Valencia CA). Synthesis of cDNA was performed as described previously (Takimoto et al., 2002). These primers were designed to detect splicing variants in different sizes (Table 1). PCR was done under the following conditions: denature at 94 °C for 5 seconds, annealing at 64 °C for 5 seconds and extension at 72 °C for 60 seconds for 28 cycles (22 cycles for GAPDH), and final extension at 72 °C for 4 minutes. PCR products were separated on a 5% polyacrylamide gel and stained with ethidium bromide for visualization. Control PCRs using cDNA made without reverse transcriptase generated no visible products.

Immunohistochemistry

Rats were perfused transcardially with saline followed by 4% paraformaldehyde in 0.1 M phosphate buffer, and L4 and L5 DRGs were then removed. Tissues were post-fixed in 4% paraformaldehyde in 0.1 M phosphate buffer overnight, and then cryoprotected in 10, 20, and 30% series of sucrose in 0.01 M phosphate buffered saline. Tissue was cut in 5 or 10 μm thick sections for subsequent histological examination. Immunohistochemical analyses were performed on tissue sections obtained from different DRGs.

The general expression pattern of Kv4 subunits were examined in L4 or L5 DRG sections. After quenching of endogenous peroxidase activity by using 3% hydrodioxyde, the tissue sections were incubated with 5% of bovine serum albumin in 0.01 M phosphate-buffered saline at room temperature for 30 minutes. The sections were then probed with antibody against Kv pore-forming subunits anti-Kv 4.3 antibody at 1: 200; NeuroMab Facility, Davis, California) in 5% of bovine serum albumin and 0.3% Triton X-100 in 0.01 M phosphate-buffered saline overnight at 4 °C. Kv immunoreactive proteins were detected with 5 mg L^{-1} (1:200) biotin-conjugated anti-mouse IgG (Jackson ImmunoResearch Laboratories, Inc., West Grove, Pennsylvania) at room temperature for 1 hour and then reacted with avidin–biotin peroxidase complex (VECTSTAIN Elite ABC Kit, Vector Laboratories, Inc., Burlingame, California) at room temperature for 30 minutes. The probed sections were washed with 0.02 M Tris–HCl pH 7.4 and incubated with diaminobenzidine (DAB Substrate kit, Vector Laboratories, Inc.). For immunofluorescence staining, anti-Kv4.3 (1:200) or anti-KChIP3 (1: 200) antibody (NeuroMab Facility) in 5% of bovine serum albumin and 0.3% Triton X-100 in 0.01 M phosphate-buffered saline were applied overnight at 4 °C. The sections were incubated with 5 mg L^{-1} (1:200) biotin-conjugated goat anti-mouse IgG (Jackson ImmunoResearch Laboratories, Inc.) at room temperature for 2 hours and then reacted with 2.7 mg L^{-1} Alexa Fluor 488-streptavidin conjugate (1:750) (Molecular probes Inc., Eugene, Oregon) at room temperature for 2 hours.

In situ hybridization

A portion of rat Kv4.1, Kv4.3, DPP6 and DPP10 cDNAs was obtained by RT-PCR and cloned into a topoisomerase-based vector (pCR2.1-TOPO or pCRII-TOPO, Invitrogen) for RNA probe synthesis. Primers used for the cloning were as follows: Kv4.1 5′-cacagacgagctaactttcag-3′ and 5′-tcacagggaagagatcttgac-3′ (GenBank ID: 116695); Kv4.3 5′-tg ggttatcctatcttgtgga-3′ and 5′-ttacaagacagagaccttgac-3′ (GenBank ID: 65195); DPP6, 5′-agcaatgacaacatccagtc-3′and 5′-agtaccatccaccacgagc-3′ (GenBank ID: 29272); DPP10 5′-gagcaaattacggtgcgcgact-3′ and 5′-cttcatctattattagtagaagagc-3′ (GenBank accession # AY557199). Digoxigenin-labeled RNA probes were synthesized using linearized plasmids with T7 and SP6 RNA polymerases.

In situ hybridization was performed according to the procedure described previously (Tatsumi et al., 2005) and the signal was detected by dig-NBT/BCIP system. Briefly, after rehydration with 0.1 M phosphate buffer, the sections of L4 DRG were treated with 0.2 M HCl. The sections were then treated with 10 μg mL^{-1} proteinase K in 50 mM Tris–HCl and 5 mM EDTA and then fixed with 4% formaldehyde in 0.1 M phosphate buffer. The sections were acetylated by 0.25% acetic anhydride in 0.1 M triethanolamine, dehydrated by ethanol series (70, 95 and 100%), defatted in chloroform, rinsed with ethanol, and dried. Denatured labeled RNA probes were applied and hybridized at 50 °C. Remaining probes were eliminated with RNase A, followed by washing with 50% formamide in sodium chloride sodium citrate. Digoxigenin-labeled probes were processed by anti-digoxigenin antibody-conjugated alkaline phosphatase, and visualized using nitro-blue tetrazolium chloride/5-bromo-4-chloro-3′-indolyphosphate p-toluidine salt.

Histological analysis

Sections stained by *in situ* hybridization technique and immunohistochemistry with DAB were viewed under an Olympus BX51 Microscope (OLYMPUS Corp., Tokyo, Japan) in bright field. Fluorescent images were captured on an Olympus FluoView 1000 confocal microscope (OLYMPUS Corp., Tokyo, Japan). Randomly selected two sections from each DRG at more than 50 μm intervals were used for counting of positively stained cells to avoid double counting of cells. Cross-sectional areas of all neuronal profiles, in which nuclei were identified, were measured by using Scion Image (Scion Corp., Frederick, Maryland). Neuronal profiles were then divided into small-, medium- and large-sized neuronal populations based on the

Table 1
Primers used in the RT-PCR study.

Gene	GenBank accession no.	Sequence 5′-3′	Position	Product sizes
KChIP1	AY082657	atgggggccgtcatgggcac accacaccactggggcactcg	1-20 239-219	KChIP1a 239 KChIP1b 206
KChIP2	XM_342059	gctcctatgaccagcttacgg cctcgttgacaatcccactgg	275-295 598-578	KChIP2a 324 KChIP2b 270 KChIP2c 174
KChIP3	NM_032462	aggctcagacagcagtgaca gggggaagaactgggaataa	197-216 393-374	197
KChIP4	AF345444	agatgaacgtgagaagggtgga gtgcatatgtggtggagtctc	376-397 753-733	KChIP4a 378 KChIP4b 276
GAPDH	NM_017008	gccatcactgccactcag gtgagcttcccgttcagc	608-625 739-756	149

Please cite this article as: Matsuyoshi H, et al, Distinct cellular distributions of Kv4 pore-forming and auxiliary subunits in rat dorsal root ganglion neurons, Life Sci (2012), doi:10.1016/j.lfs.2012.07.007

area size (area<600 μm^2, 600 μm^2<area<1200 μm^2 and area> 1200 μm^2, respectively). The staining intensity was rated on a four point scale, from completely negative (grade 0) to intense staining (grade 3), and the neurons that exhibited grades 2 or 3 were regarded as positively stained cells. The number of positively stained cells as well as the total DRG neurons was counted, and the percent ratio of positively stained cells against the total DRG cells was calculated.

Results

Cellular distributions of Kv4 pore-forming subunits in DRGs

Previous PCR analysis suggested significant expression of Kv4.1 and Kv4.3 mRNAs in DRG neurons (Phuket and Covarrubias, 2009). We also observed abundant Kv4.1 and long-isoform of Kv4.3 transcripts, but not Kv4.2 mRNA, in L6-S1 DRGs (unpublished observation). Thus, we first examined the cellular distributions of the two pore-forming subunits, Kv4.1 and Kv4.3. Since commercial anti-Kv4.1 antibodies appeared less suitable for immunohistochemistry, we used *in situ* hybridization to test for differential distributions of Kv4.1 and Kv4.3 in DRG neurons (Fig. 1). Antisense Kv4.3 probe preferentially stained small-sized neuronal cell bodies (Fig. 1B). Kv4.3 transcript-positive cells represented approximately 32.8% of DRG neurons (total 4 sections), equivalent to that of the corresponding channel proteins (33.8%). Most Kv4.3 mRNA-positive cells were less than 900 μm^2 in cell area size. Consistent with mRNA distribution, anti-Kv4.3 antibody stained small-sized neuronal cell bodies (data not shown). Kv4.3 protein-positive cells represented approximately 33.8% of DRG neurons.

In contrast, antisense Kv4.1 probe detected DRG neurons in various sizes (Fig. 1A). Kv4.1 mRNA-positive cells represented 59.5 % of DRG neurons (total 4 sections) and were distributed in all sizes. Thus, the two Kv4 pore-forming subunits are differentially distributed in DRG neurons.

Cellular distributions of Kv4 channel auxiliary subunits

Kv4 pore-forming subunits may be associated with the two distinct types of auxiliary subunits that significantly alter channel expression and gating. We first tested expression of KChIP1-4 mRNAs by RT-PCR analysis (Fig. 2A). All four gene transcripts were abundant in the brain, whereas only KChIP3 mRNA was significant in L6-S1 DRGs. Immunostaining with anti-KChIP3 antibody showed that KChIP3 proteins were prominent in a subset of medium to large-sized neuronal cell bodies (Fig. 2B). Staining with anti-Kv4.3 antibody of adjunct sections suggested that Kv4.3 and KChIP3 are not colocalized in the same cells (Fig. 2B).

We next examined cellular distribution of the other type of Kv4 channel auxiliary subunits, DPP6 and DPP10. Our previous study demonstrated abundant mRNA expression of these two auxiliary subunits in DRGs (Takimoto et al., 2006). Since several available antibodies against these proteins failed to provide reliable staining, we performed *in situ* hybridization analyses (Fig. 3). DPP6 mRNA was widely distributed in DRG neuronal cell bodies in all sizes (Fig. 3A), whereas DPP10 transcript was expressed mostly in small to medium-sized neurons ranging 400–1600 μm^2 of cell area size (Fig. 3B). The proportions of DPP6 and DPP10 mRNA-positive cells among DRG neurons per section were 72.8% and 27.2%, respectively (the mean of $n=2$ sections). Thus,

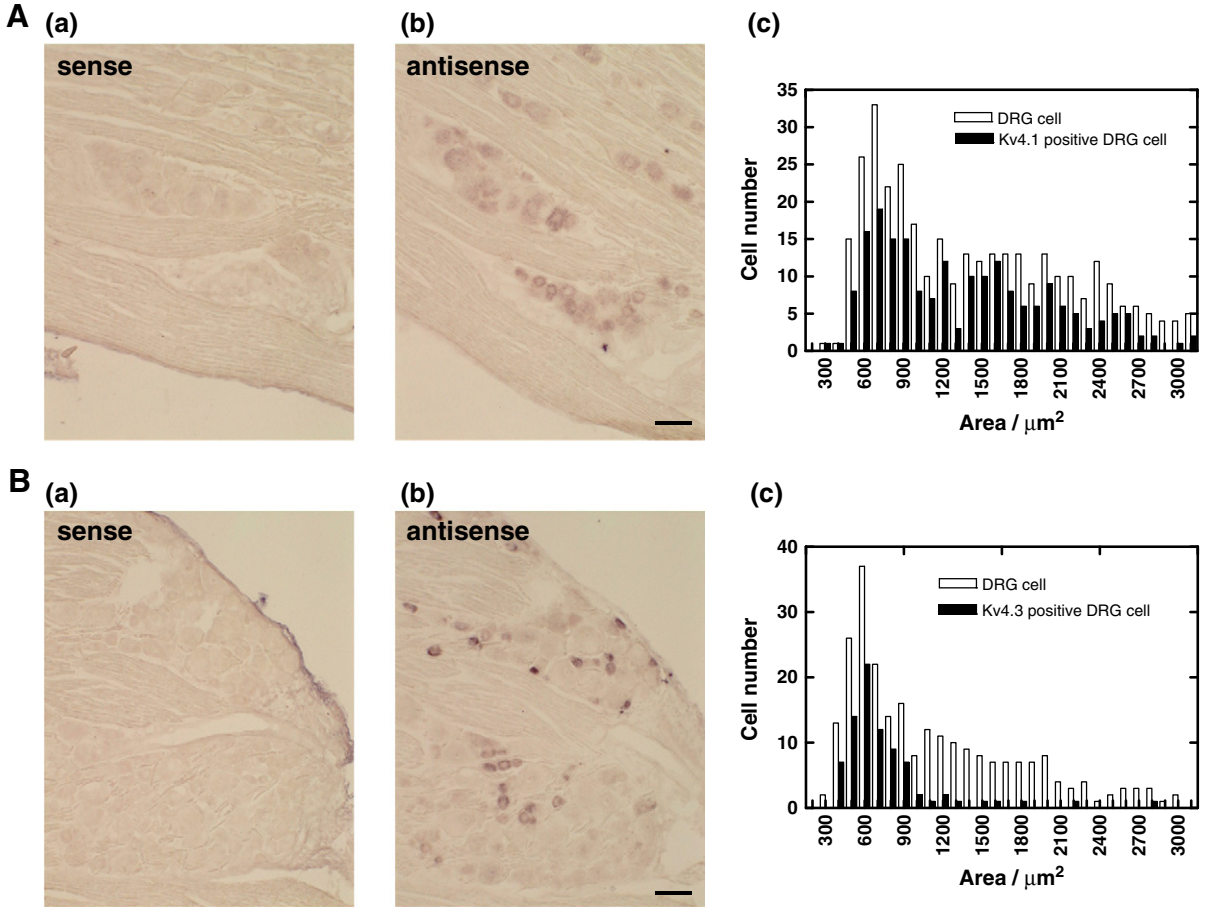

Fig. 1. Cellular distributions of Kv4.1 and Kv4.3 mRNA in rat DRGs. A. Rat DRG sections stained with Kv4.1-sense RNA probe (a) or Kv4.1-antisense RNA probe (b), are shown. Cell-size distributions are shown with filled and open columns indicating Kv4.1 mRNA-positive and total DRG neuronal cell bodies, respectively (c). B. In situ hybridization picture (a, b) and cell-size distributions (c) for Kv4.3 are shown. Scale bar, 50 μm. Bin width: 100 μm^2.

Please cite this article as: Matsuyoshi H, et al, Distinct cellular distributions of Kv4 pore-forming and auxiliary subunits in rat dorsal root ganglion neurons, Life Sci (2012), doi:10.1016/j.lfs.2012.07.007

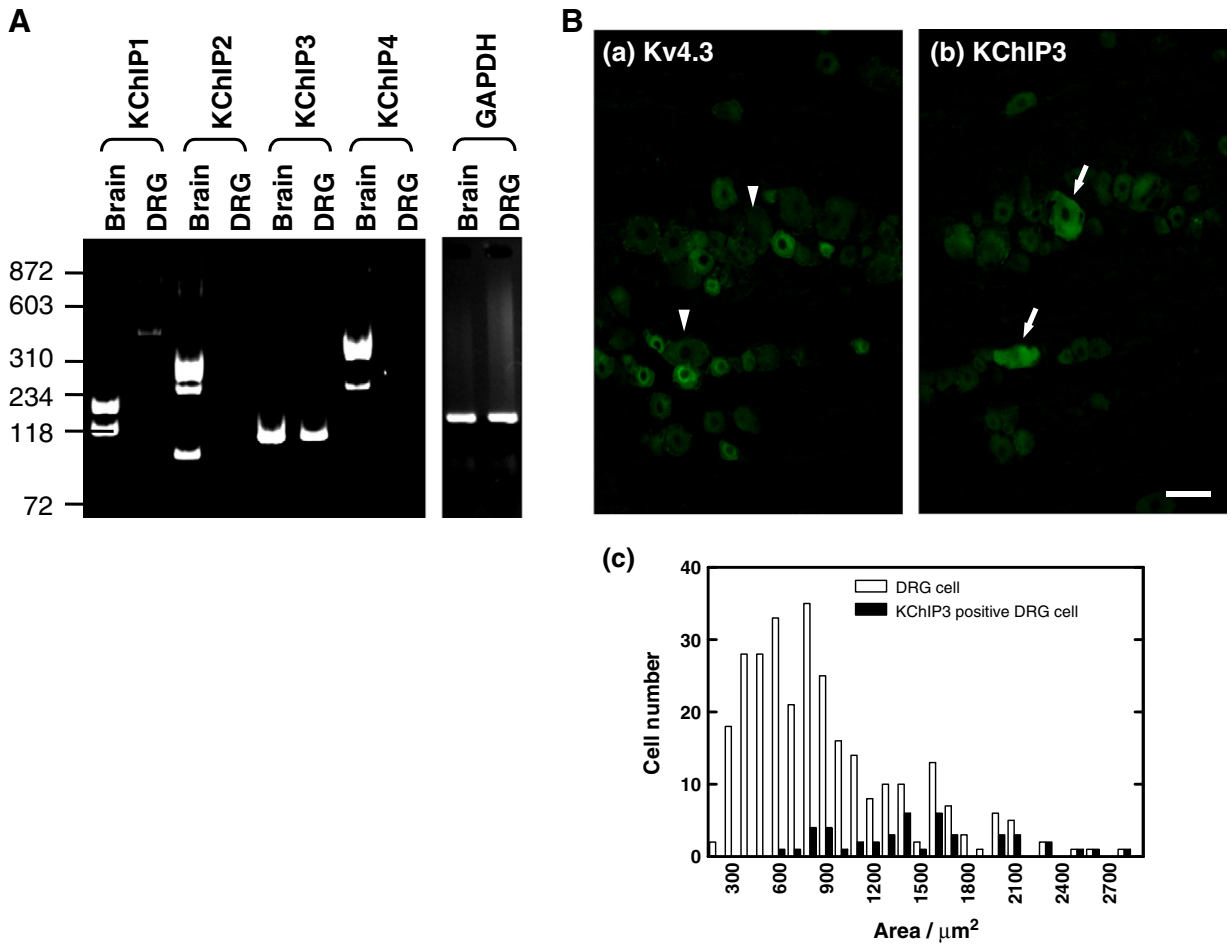

Fig. 2. Expression of KChIPs in rat DRGs. A. RT-PCR data with primers for KChIP1-4 in the brain and L6-S1 DRG are shown. Different sizes of bands represent splicing variants: KChIP1a and KChIP1b (Boland, et al., 2003); KChIP2a, KChIP2b and KChIP2c (Takimoto, et al., 2002); KChIP4 (Takimoto, et al., 2002). Note that DRGs contain only KChIP3. B. Adjacent L5 DRG sections at a 10 μm interval stained with anti-Kv4.3 antibody (a) or anti-KChIP3 antibody (b) are shown. Scale bar, 50 μm. Arrow heads (a) and arrows (b) indicate the same cells that are negative for Kv4.3 and positive for KChIP3, respectively. Cell-size distributions are shown with filled and open columns indicating KChIP3 protein-positive and total DRG neuronal cell bodies, respectively (c). Bin width: 100 μm^2.

the two auxiliary subunits differently contribute to the production of Kv4 channel complexes in DRG neurons with different sizes.

Discussion

DRGs contain cell bodies for heterogeneous populations of primary afferent neurons. These neurons may be categorized by cell body sizes and innervating tissues. Aα/β-fiber neurons with large-sized cell bodies generally carry mechanical information, whereas small-sized cell bodies correspond to C and Aδ-fiber neurons that are responsible for pain sensation. The latter small-sized neurons are also implicated in the development of chronic pain. In this study, we determined the cellular distribution of Kv4 pore-forming subunits and their associating auxiliary subunits in DRG neurons. We found that Kv4.1 mRNA is widely expressed in DRG neurons with various cell body sizes. Similarly, mRNA for the auxiliary subunit DPP6 is ubiquitous in neurons with various cell body sizes, whereas DPP10 transcript is more concentrated in small-sized neurons. In addition, KChIP3 protein seems more abundant in medium to large-sized neurons. These new findings suggest that Kv4.1 channel complexes containing DPP6 and KChIP3 contribute to K_A currents in medium to large-sized A-fiber neurons, whereas Kv4.3 channel complexes containing DPP10 may be responsible for K_A currents in small-sized C-fiber somatic neurons.

DRG neurons are known to contain two types of K_A currents with distinct kinetics (fast vs. slow-inactivating) and toxin sensitivities. Fast-inactivating K_A current is sensitive to heteropodatoxins and phrixotoxins that influence the gating of Kv4 channels, but not Kv1 or Kv2 channels (Sanguinetti et al., 1997; Diochot et al., 1999; Escoubas et al., 2002). Thus, it is assumed that Kv4 channel complexes are responsible for the fast K_A current. While fast-inactivating K_A current is prominent in medium to large-cell sized A-fiber neurons (Gold et al., 1996; Yoshimura and de Groat, 1996), it may also be present in a subset of small-sized C-fiber neurons. Our immunostaining and *in situ* hybridization clearly showed the presence of Kv4.3 pore-forming subunit and DPP10 auxiliary subunit in small-sized DRG neurons. We have recently observed that phrixotoxin-sensitive K_A current is prominent in somatic sensory neurons, but not bladder afferent cells (unpublished observation). Thus, Kv4.3 pore-forming and DPP10 ancillary subunits may contribute to the formation of fast K_A channels in somatic C-fiber neurons. In addition, Kv4.1 mRNA has been detected in dissociated, small to medium-cell sized DRG neurons (Phuket and Covarrubias, 2009). Our *in situ* hybridization study further demonstrated that Kv4.1 mRNA is expressed not only in small to medium-sized DRG neurons, but in DRG neurons with various cell sizes. Therefore, it is likely that this Kv4.1 pore-forming subunit may also participates in forming fast K_A channels in small-sized DRG neurons.

Kv4 channels may simultaneously contain the two distinct auxiliary subunits, KChIPs and DPP6/10. In the brain, immunoprecipitation studies indicated ternary channel complexes containing the two types of auxiliary subunits (Jerng et al., 2005; Amarillo et al., 2008).

Please cite this article as: Matsuyoshi H, et al, Distinct cellular distributions of Kv4 pore-forming and auxiliary subunits in rat dorsal root ganglion neurons, Life Sci (2012), doi:10.1016/j.lfs.2012.07.007

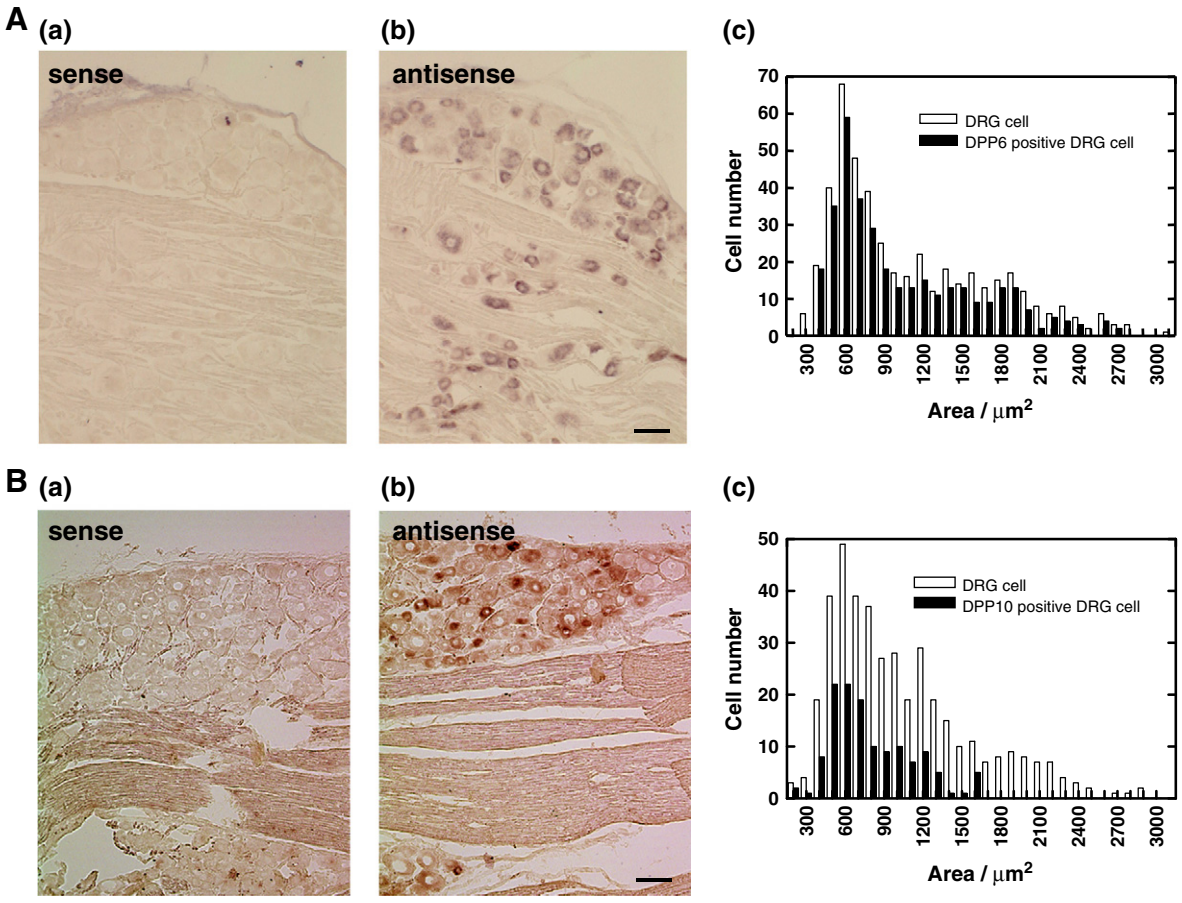

Fig. 3. Cellular distributions of DPP6 or DPP10 mRNA in rat DRGs. A. Rat DRG sections stained with DPP6-sense (a) or antisense RNA probe (b), are shown. Cell-size distributions are shown with filled and open columns indicating DPP6 mRNA-positive and total DRG neuronal cell bodies, respectively (c). B. In situ hybridization picture (a, b) and cell-size distributions (c) for DPP10 are shown. Scale bar, 50 μm. Bin width: 100 μm^2.

However, our RT-PCR analysis and *in situ* hybridization suggest that some Kv4 channel complexes may not contain KChIPs. RT-PCR analysis detected a high level of KChIP3 without apparent expression of other three KChIPs in DRGs, whereas all four auxiliary subunit mRNAs were abundant in the brain. Moreover, immunohistochemistry indicated that KChIP3 protein is present in medium to large-sized neurons, but not in small-sized cells. A simple explanation for these observations is that Kv4 channel complexes in small-sized DRG neurons consist of Kv4.1/Kv4.3 and DPP6/10, but not any KChIPs, whereas Kv4 channel complexes in medium to large-sized DRG neurons consist of Kv4.1, DPP6 and KChIP3. Heterologous expression studies suggest that KChIPs and DPP6/10 somewhat play redundant roles in raising expression of the associated pore-forming subunits and inducing faster recovery from inactivation. Therefore, it is possible that a subset of small-sized C-fiber neurons contain Kv4 channel complexes without any KChIPs.

Sensory neuron-type selective expression of different channel subunits may provide the basis for the development of new therapeutic strategy or drugs for chronic pain and other disorders. We have previously showed that reduced expression of Kv1.4 subunits is associated with hyperexcitability of DRG neurons in an animal model of bladder inflammation (Hayashi et al., 2009). In contrast to visceral pain, less attention is focused on molecular correlates for Kv channel plasticity in primary afferents that transmit somatic pain, such as arthritis and chronic back pain. Further studies on alterations in the expression of Kv4 pore-forming and auxiliary subunits and functional properties of Kv4-mediated K_A currents could identify the molecular correlates that contribute to somatic pain conditions.

Conclusion

Kv4 channel complexes in small-sized, somatic DRG neurons consist of Kv4.1/Kv4.3 and DPP6/10, but not any KChIPs, whereas Kv4 channel complexes in medium to large-sized DRG neurons consist of.Kv4.1, DPP6 and KChIP3.

Conflict of interest statement

None.

Acknowledgements

This work was supported by grants from the National Institute of Health (DK057267 and DK088836), the Department of Defense (SC100134 and PR110326) and the Ministry of Education, Science, Sports and Culture of Japan (22591798).

References

Amarillo Y, De Santiago-Castillo JA, Dougherty K, Maffie J, Kwon E, Covarrubias M, et al. Ternary Kv4.2 channels recapitulate voltage-dependent inactivation kinetics of A-type K+ channels in cerebellar granule neurons. J Physiol 2008;586:2093–106.

An WF, Bowlby MR, Betty M, Cao J, Ling H, Mendoza G, et al. Modulation of A-type potassium channels by a family of calcium sensors. Nature 2000;403:553–6.

Boland LM, Jiang M, Lee SY, Fahrenkrug SC, Harnett MT, O'Grady SM. Functional properties of a brain-specific NH2-terminally spliced modulator of Kv4 channels. Am J Physiol Cell Physiol 2003;285:C161–70.

Chien L-Y, Cheng J-K, Chu D, Cheng C-F, Tsaur M-L. Reduced expression of A-type potassium channels in primary sensory neurons induces mechanical hypersensitivity. J Neurosci 2007;27:9855–65.

Please cite this article as: Matsuyoshi H, et al, Distinct cellular distributions of Kv4 pore-forming and auxiliary subunits in rat dorsal root ganglion neurons, Life Sci (2012), doi:10.1016/j.lfs.2012.07.007

Diochot S, Drici MD, Moinier D, Fink M, Lazdunski M. Effects of phrixotoxins on the Kv4 family of potassium channels and implications for the role of Ito1 in cardiac electrogenesis. Br J Pharmacol 1999;126:251–63.
Escoubas P, Diochot S, Célérier ML, Nakajima T, Lazdunski M. Novel tarantula toxins for subtypes of voltage-dependent potassium channels in the Kv2 and Kv4 subfamilies. Mol Pharmacol 2002;62:48–57.
Gold MS, Shuster MJ, Levine JD. Characterization of six voltage-gated K+ currents in adult rat sensory neurons. J Neurophysiol 1996;75:2629–46.
Hall A, Stow J, Sorensen R, Dolly JO, Owen D. Blockade by dendrotoxin homologues of voltage-dependent K+ currents in cultured sensory neurons from neonatal rats. Br J Pharmacol 1994;113:959–67.
Hayashi Y, Takimoto K, Chancellor MB, Erickson KA, Erickson VL, Kirimoto T, et al. Bladder hyperactivity and increased excitability of bladder afferent neurons associated with reduced expression of Kv1.4 α-subunit in rats with cystitis. Am J Physiol Regul Integr Comp Physiol 2009;296:R1661–70.
Holmqvist MH, Cao J, Hernandez-Pineda R, Jacobson MD, Carroll KI, Sung MA, et al. Elimination of fast inactivation in Kv4 A-type potassium channels by an auxiliary subunit domain. Proc Natl Acad Sci U S A 2002;99:1035–40.
Jerng HH, Qian Y, Pfaffinger PJ. Modulation of Kv4.2 channel expression and gating by dipeptidyl peptidase 10 (DPP10). Biophys J 2004;87:2380–96.
Jerng HH, Kunjilwar K, Pfaffinger PJ. Multiprotein assembly of Kv4.2, KChIP3 and DPP10 produces ternary channel complexes with I_{SA}-like properties. J Physiol 2005;568: 767–88.
Kostyuk PG, Veselovsky NS, Fedulova SA, Tsyndrenko AY. Ionic currents in the somatic membrane of rat dorsal root ganglion neurons-III. Potassium currents. Neuroscience 1981;6:2439–44.
Morohashi Y, Hatano N, Ohya S, Takikawa R, Watabiki T, Takasugi N, et al. Molecular cloning and characterization of CALP/KChIP4, a novel EF-hand protein interacting with presenilin 2 and voltage-gated potassium channel subunit Kv4. J Biol Chem 2002;277:14965–75.
Nadal MS, Ozaita A, Amarillo Y, de Miera EV-S, Ma Y-L, Mo W-J, et al. The CD26-related dipeptidyl aminopeptidase-like protein DPPX is a critical component of neuronal A-type K^+ channels. Neuron 2003;37:449–61.
Patel SP, Campbell DL, Strauss HC. Elucidating KChIP effects on Kv4.3 inactivation and recovery kinetics with a minimal KChIP2 isoform. J Physiol 2002;545(Pt 1):5-11.
Phuket TR, Covarrubias M. Kv4 channels underlie the subthreshold-operating A-type K-current in nociceptive dorsal root ganglion neurons. Front Mol Neurosci 2009;2:3.
Rasband MN, Park EW, Vanderah TW, Lai J, Porreca F, Trimmer JS. Distinct potassium channels on pain-sensing neurons. Proc Natl Acad Sci U S A 2001;98:13373–8.
Ren X, Hayashi Y, Yoshimura N, Takimoto K. Transmembrane interaction mediates complex formation between peptidase homologues and Kv4 channels. Mol Cell Neurosci 2005;29:320–32.
Rosati B, Pan Z, Lypen S, Wang HS, Cohen I, Dixon JE, et al. Regulation of KChIP2 potassium channel beta subunit gene expression underlies the gradient of transient outward current in canine and human ventricle. J Physiol 2001;533(Pt 1):119–25.
Sanguinetti MC, Johnson JH, Hammerland LG, Kelbaugh PR, Volkmann RA, Saccomano NA, et al. Heteropodatoxins: peptides isolated from spider venom that block Kv4.2 potassium channels. Mol Pharmacol 1997;51:491–8.
Takimoto K, Yang EK, Conforti L. Palmitoylation of KChIP splicing variants is required for efficient cell surface expression of Kv4.3 channels. J Biol Chem 2002;277:26904–11.
Takimoto K, Hayashi Y, Ren X, Yoshimura N. Species and tissue differences in the expression of DPPY splicing variants. Biochem Biophys Res Commun 2006;348:1094–100.
Tatsumi K, Haga S, Matsuyoshi H, Inoue M, Manabe T, Makinodan M, et al. Characterization of cells with proliferative activity after a brain injury. Neurochem Int 2005;46:381–9.
Yoshimura N, de Groat WC. Characterization of voltage-sensitive Na+ and K+ currents recorded from acutely dissociated pelvic ganglion neurons of the adult rat. J Neurophysiol 1996;76:2508–21.
Yoshimura N, White G, Weight FF, de Groat WC. Different types of Na^+ and A-type K^+ currents in dorsal root ganglion neurones innervating the rat urinary bladder. J Physiol 1996;494:1-16.

Please cite this article as: Matsuyoshi H, et al, Distinct cellular distributions of Kv4 pore-forming and auxiliary subunits in rat dorsal root ganglion neurons, Life Sci (2012), doi:10.1016/j.lfs.2012.07.007